Unclassified

SECURITY CLASSIFICATION OF THIS PAGE (When Data Entered)

REPORT DOCUMENTATION PAGE	READ INSTRUCTIONS BEFORE COMPLETING FORM
1. REPORT NUMBER: Technical Report #1	2. GOVT ACCESSION NO. AD-A120891 / 3. RECIPIENT'S CATALOG NUMBER
4. TITLE (and Subtitle): Tectonics of China	5. TYPE OF REPORT & PERIOD COVERED: Semi-Annual Technical Report 1 October 1976-31 March 1977
	6. PERFORMING ORG. REPORT NUMBER
7. AUTHOR(s): James Ni	8. CONTRACT OR GRANT NUMBER(s): AFOSR 77-3170
9. PERFORMING ORGANIZATION NAME AND ADDRESS: Department of Geological Sciences, Cornell University, Ithaca, New York 14853	10. PROGRAM ELEMENT, PROJECT, TASK AREA & WORK UNIT NUMBERS: Project Task AO 3291-1
11. CONTROLLING OFFICE NAME AND ADDRESS: Air Force Office of Scientific Research, 1400 Wilson Blvd., Arlington, Virginia 22209	12. REPORT DATE: April 28, 1977
	13. NUMBER OF PAGES
14. MONITORING AGENCY NAME & ADDRESS (if different from Controlling Office): same	15. SECURITY CLASS. (of this report): unclassified
	15a. DECLASSIFICATION/DOWNGRADING SCHEDULE

16. DISTRIBUTION STATEMENT (of this Report)

Approved for public release; distribution unlimited

17. DISTRIBUTION STATEMENT (of the abstract entered in Block 20, if different from Report)

18. SUPPLEMENTARY NOTES

none

19. KEY WORDS (Continue on reverse side if necessary and identify by block number)

Intraplate Earthquakes, LANDSAT Imagery, Fault Plane Solutions, Tibetan Plateau

20. ABSTRACT (Continue on reverse side if necessary and identify by block number)

Contemporary tectonics and earthquakes are being studied in several areas in China by analysis of seismicity, geomorphology, igneous activity, and faulting. Geologic information is interpreted from LANDSAT imagery. Information from fault plane solutions and LANDSAT imagery indicates that the Tibetan Plateau is in east-west extension. Study of the Tien Shan earthquake sequences by the JHD technique shows a northwest-trending fault plane. The fault plane solution of the February 4, 1975 Haicheng earthquake and aftershock sequence indicates a rupture along the east-west trending fault plane.

DD FORM 1 JAN 73 1473 EDITION OF 1 NOV 65 IS OBSOLETE

Unclassified

SECURITY CLASSIFICATION OF THIS PAGE (When Data Entered)

Form Approved
Budget Bureau No. 22-R0293

Semi-Annual Technical Report
for period 1 October 1976 - 31 March 1977

to

Air Force Office of Scientific Research

from

Department of Geological Sciences
Cornell University
Ithaca, New York 14853

Title of Proposal:	Contemporary Tectonics of China
Report Prepared by:	James Ni
Sponsored by:	Advanced Research Projects Agency ARPA Order No. 3291
Program Code:	7F10
Effective Date of Contract:	1 October 1976
Contract Expiration Date:	30 September 1977
Amount of Contract Dollars:	$30,000
Contract Number:	AFOSR 77-3170
Program Manager:	William J. Best 202-693-0162
Principal Investigator:	Jack E. Oliver 607-256-2377 Bryan L. Isacks 607-256-2307

Jack E. Oliver, Principal Investigator

Bryan L. Isacks, Principal Investigator

Sponsored by
Advanced Research Projects Agency (DOD)
ARPA Order No. 3291
Monitored by AFOSR Under Grant #AFOSR 77-3170

Technical Problem

Although a successful theoretical and empirical framework has been developed for understanding seismicity near lithospheric plate boundaries, earthquakes occurring within these boundaries remain an enigma. Intraplate earthquakes are less common than seismic events in active tectonic regions, but they are known to reach large magnitudes. In general, we do not understand why or how such shocks occur, what geological features they are asscciated with, where they may be expected to occur in the future, or why their seismograms in many ways more closely resemble those of buried nuclear explosions than those of shocks in the major seismic belts. An increased understanding of intraplate earthquakes is essential in the planning of major constructions such as dams, nuclear power plants and other large structures. It is also necessary for the safety of thousands or even millions of lives. The recent successes in earthquake prediction by the Chinese indicate that it would be of value to the United States to understand seismicity in China because their methods used in predicting large intraplate seismic events can be applied to predicting large seismic events in the United States. An increased understanding of intraplate earthquakes can also improve our ability to discriminate between natural events and nuclear explosions.

General Method

In order to circumvent the limitations placed on studies of Chinese seismicity by the infrequent occurrence of intraplate earthquakes, data from historical records of earthquakes, instrumentally located epicenters, fault plane solutions, and geologic evidence for long-term movements are incorporated and evaluated in this study. Literature reviews on Tibet have been completed and others are being compiled. LANDSAT data is particularly valuable in studying the tectonics of China because ground observations by western scientists are not possible. The imagery has revealed previously unknown, large, strike-slip faults in China. Ponding of streams and offset of alluvium on these and other faults are evidence that the faults are active. We are continuing to obtain and analyze LANDSAT imagery. The mapping of geologic features is being integrated with fault plane solutions, seismicity patterns, and regional stress patterns.

Earthquake swarms and aftershock sequences are being studied with the Joint Hypocenter Determination (JHD) technique to yield very accurate relative locations. Fault planes may be determined with this method, thereby

removing the ambiguity of the choice of fault plane from a fault plane solution. Data from the World Wide Network of Seismograph Stations (WWNSS) are being used for the JHD method. First P motions from long-period seismograms and S wave polarizations are being used to construct fault plane solutions. These fault plane solutions and the previously determined ones will improve the understanding of local stress patterns and regional tectonics.

In order to evaluate the generality of the conclusions reached in the detailed research concerning China, results of similar studies in the eastern United States are being examined so that any fundamental relationships common to both areas can be understood.

Technical Results

Preliminary results of the research sponsored by this contract are a study of Tien Shan earthquake swarms and aftershock sequences by the JHD technique, and fault plane solution of the February 4, 1975 Hai-cheng earthquake.

A detailed study of the Tibetan Plateau has been completed. Interpretation of a mosaic of LANDSAT imagery, literature research, seismicity, and fault plane solutions suggests the importance of east-west regional tensional tectonics in the central and western Tibetan Plateau in addition to the better known compressional tectonics that probably result from the collision of the Indian and Eurasian plates. North-south trending en-echelon normal faults are observed on LANDSAT imagery. A few east-west trending normal faults are observed in areas near large strike-slip faults and are interpreted as secondary faults. The seismicity of the central and western Tibetan Plateau is relatively high for an intraplate area and earthquake swarms are common. Based on good azimuthal distribution of teleseismic stations, 45% of all earthquakes located by the International Seismological Centre (ISC) from 1961 to 1975 were selected. These epicenters show a close relationship to the fault traces which are interpreted from LANDSAT imagery. Fault plane solutions, some newly determined, also show some normal faulting with the orientation of the T-axis in approximately the east-west direction. Late Tertiary and Quaternary volcanics are observed on LANDSAT imagery. Most observed volcanic landforms are extensively eroded. However, younger, probably Quaternary, volcanics are observed sporadically throughout the central and western Tibetan Plateau.

LATE CENOZOIC EXTENSIONAL TECTONICS OF THE TIBETAN PLATEAU

by James Ni

Abstract

Interpretation of a mosaic of LANDSAT imagery, literature research, seismicity, and fault plane solutions suggest the existence of east-west regional tensional tectonics in the Tibetan Plateau in addition to the better known compressional tectonics that probably result from the collision of the Indian and Eurasian plates. The east-west crustal extension can be explained by a combination of mechanical disequilibrium and wedging effect. The recent volcanism is explained as the result of the crustal extension.

INTRODUCTION

The Tibetan Plateau, situated north of the Himalayan foldbelt, has been under complex deformation since the collision of the Indian and Eurasian plates in late Eocene (Ganser, 1964; Dewey and Burke, 1973; Molnar and Tapponnier, 1975). Because very little published geological and geophysical data on the Tibetan Plateau is available, the deformation and uplift of the Tibetan Plateau and its relationship to the plate convergence is still poorly understood. Available data indicate that deformation is accompanied by strike-slip faulting (Molnar and Tapponnier, 1975; York and others 1976), thrusting in the upper crust, and probably ductile creep at a deeper level (Dewey and Burke, 1973; Burke and others, 1974). Normal faulting in northern Tibetan Plateau interpreted from LANDSAT imagery (Tapponnier and Molnar, 1977), and north-south trending Thakkola graben situated in the Tibetan Himalayas (Colchen, 1974), display evidence of Quaternary activity. Normal fault plane solutions (Fitch, 1970; Molnar and others, 1973; Tapponnier and Molnar, 1977) in the Tibetan Plateau also indicate east-west tension. In an attempt to clarify the late Cenozoic tectonics of the Tibetan Plateau, this paper will present a detailed study of the seismicity, fault plane solutions, and geological features interpreted from LANDSAT imagery as it pertains to the structure and tectonics of the Tibetan Plateau.

GENERAL BACKGROUND OF TIBETAN PLATEAU

The area described by Powell and Conaghan (1975) as the Tibetan Plateau coincides with that area presently named the Chinghai-Tibetan Plateau on the geographic map by the Chinese Academy of Sciences. This region is bounded on the north by the Kunlun, Astin Tagh, and Nan Shan mountains, by the High Himalayas on the south, by the north-south trending ranges that flank the Szechwan and Yunnan basins on the east, and by the Karakoram mountain on the west. In this paper the Tibetan Plateau will be defined as that area averaging above 5000 meters in elevation. This area, somewhat smaller than the Chinghai-Tibetan Plateau, is bounded on the south by the High Himalayas, on the north by the Kunlun mountain, on the east by the approximate boundary where high plateau lakes begin to disappear (about 91°-93°N), and on the west by the Karakoram mountain (Fig. 1).

The Tibetan Plateau may be divided into 4 tectonic units (Fig. 1), which will be discussed from south to north. (1) The Tibetan Himalayas are composed of Precambrian to Mesozoic shelf sediments and Cenozoic ophiolite-flysch-molasse facies. The eugeosynclinal flysch-molasse facies have been thrust to the south (Ganser, 1964). Neogene, granite intrusives are also extensively distributed in the south. (2) The Nyenchhen Thangla Basin is characterized by Paleozoic metamorphic rocks and extensive Mesozoic granitoid batholiths (Chang, 1959). A band, averaging 120 km wide, of andesitic volcanics of the late Cretaceous to early Paleocene age in the south (Geologic map of China, 1976) probably represents an Andean-type arc north of the subducting Indian Plate about 65 m.y. ago. A smaller band of Neogene to Quaternary volcanics lie north of the older volcanic band. (3) The Chang Thang Platform is composed of Mesozoic sedimentary rocks. The Mesozoic sediments have been folded intensely in the south.

Quaternary lake and alluvial deposits are found throughout this region. (4) The Kunlun Foldbelt is composed of Paleozoic and Precambrian metamorphic rocks that were extensively folded during the Hercynian orogeny. Mesozoic land facies molasse, banded with coal beds (Change, 1959), occur within the Foldbelt. A few andesitic and trachytic volcanics are found in some parts of the Cretaceous systems (Chang, 1959). The Cenozoic sediments are primarily land facies basin deposits.

Reliable geophysical data for the Tibetan Plateau are scarce. Low Bouguer gravity and near zero free air gravity anomaly are reported by Chang and others (1976), which suggest thicker than normal crust and isostatic equilibrium of the Tibetan Plateau. No refraction studies are published to our knowledge. Interpretation of velocity sections from an explosion reflection study at the eastern Tsidam Basin indicates a crust about 43 km. thick (Teng and others, 1974). Since the Tsidam Basin is outside of the Tibetan Plateau, it does not constrain the crustal thickness in the Tibetan Plateau. Studies of surface wave dispersion data show a possible 65 to 70 km thickness of crust under the Tibetan Plateau (Gupta and Nasrain, 1967; Tung, 1975; Bird and Toksoz, 1977). Studies of surface waves propagation suggest high attenuation in the mantle beneath Tibet (Molnar and Oliver, 1969; Ruzaikin and others, 1977).

LANDSAT IMAGERY

The Tibetan Plateau, a largely unmapped area, provides a good example of the practical use of LANDSAT imagery for obtaining regional geological and tectonic information. Since the launching of LANDSAT, its imagery has been used by several investigators dealing with Quaternary tectonics and seismicity. For example, recent work in intraplate tectonics in Asia has revealed the existence of large Cenozoic tectonic features: folds, thrust and normal faults and especially very large strike-slip faults (Bonilla and Allen, 1975; Molnar and Tapponnier, 1975; York and others, 1976). The mosaic constructed by York and others (1976) at 1:1,000,000 scale, composed of black and white, band 7 (near infrared, 0.8 to 1.1 μm wavelength) is used for this study. The information extracted from this mosaic was photographically reduced to 1:4,000,000 scale and this version was used as the base map.

Lineaments are interpreted as Quaternary faults primarily based on linearity, sharpness of a scarp, and presence of a topographic, tonal or textural difference across the lineament. Characteristics of different types of faulting can be inferred from their geomorphology. Normal faults are indicated by the sharp broken and en echelon fault traces with average segment lengths of 10 to 20 km. The widths of larger grabens are 10-15 km. Smaller grabens are 5-10 km in width and some tens of km long (Fig. 3a, b). Although normal faults of the Tibetan Plateau have not been previously mapped, close comparison with known normal fault patterns in western U. S. (Fig. 3c) supports our interpretation. The majority of these normal faults, which strike northeast to northwest, on closer examination show individual faults tending to be crooked in map plan. Sometimes fault pattern is more nearly rhomboid or even rectilinear (Fig. 3a & b). These fault patterns are commonly distributed from 80°E to 93° E (Fig. 2).

Major strike-slip faults, similar to the San Andreas fault, are characterized by long and straight linear traces, and can often be readily identified from LANDSAT imagery. Evidence for recent motions along such faults is provided by sharp traces in the Quaternary alluvium and ponding of streams (Fig. 4). These faults were previously identified as Astin Tagh fault, Kunlun fault, and Kang Ting fault, all with left lateral displacement, and the Karakoram fault with right lateral displacement (Molnar and Tapponnier, 1975; York, et al., 1976; Tapponnier and Molnar, 1977). The right lateral Po Chu fault is identified in this paper (Fig. 2 & 5).

Recent thrust faults usually are hard to recognize from photo interpretation. Although the central Tibetan folds appear to be accompanied by thrusting as first seen from LANDSAT imagery, closer examination indicates that fault traces are not continuous. Very little tonal difference can be seen across fault faces. Therefore, we have no positive evidence to support the existence of active thrust faults in the central Tibetan foldbelt from photo interpretation although few east-west trending active faults are mapped in this region on the geologic map of China (1976). The east-west trending thrust faults situated in the Tibetan Himalayas have been recognized to be high angle faults (Ganser, 1964; Wong, 1974). These thrusts can also be identified from LANDSAT imageries.

Another land form mapped from LANDSAT imageries are the late Cenozoic volcanics. Volcanoes in various erosional stages, volcanic domes, eroded flow plateaus, and older forms such as mesas and plugs are identified (Fig. 6a, b, c). These volcanics comprise a range of time probably from late Cretaceous to Recent. The late Cretaceous and early Tertiary (65-50 my) andesitic igneous rocks cover most of the

southern Nyenchhen Thangla Basin (Kidd, 1975, Geologic map of China, 1976) (Fig. 2). Observed well eroded mesas and buttes on LANDSAT imagery are comparable to old volcanic landforms in New Mexico, U.S.A. (Fig. 7). Their age is probably 10 to 30 m.y. This is consistent with the mapped Oligocene intermediate and basic basalt from the geological map of China. Young volcanics of late Neogene to Quaternary age (less than 10 m.y.b.p.) are not extensively distributed throughout the Tibetan Plateau. Volcanic domes, cones, and flows are observed on LANDSAT imagery at places east of the Karakarom fault and north of the Nyenchhen Thanglha basin. One Quaternary volcano and a few basalt fields are observed at the vicinity of 80°E and 35°N (Fig. 2). These are located in an extensional zone which is associated with the Astin-Tagh fault.

SEISMICITY

Relatively high intraplate seismicity characterized by earthquake swarms with maximum magnitudes M-6½ is observed in the Tibetan Plateaus. Two great earthquakes ($M \geq 7.8$) occurred in 1950 and in 1951. In addition, since 1900 fifteen earthquakes with magnitudes from 7.0 to 7.8 occurred in this region (Shih and others, 1973; York and others, 1976). Historical seismic records in Tibet are non-existent mainly because of its low population. Selected events, with good azimuthal distribution of teleseismic stations and located by ISS from 1960 to 1963, by the ISC from 1964 to 1973, and by the U.S.G.S from 1973 to 1975 are shown in Figure 2. Data for events south of the Main Central Thrust and east of 97°E are not included. These selected epicenters, about 45% of reported earthquakes, represent the most accurately located epicenters. The elimination of poorly located epicenters enhances features not apparent when using all epicenters. Some of the epicenters fall on or near Quaternary fault traces deduced from LANDSAT imageries. An outstanding feature of the spatial distribution of epicenters is the lack of large magnitude events in central Tibet. The earthquake swarms are probably related to recent volcanism.

FAULT PLANE SOLUTIONS

Fault plane solutions were determined for 5 earthquakes using the first motion of P waves and some S wave polarizations recorded on long-period instruments of the world-wide standard seismograph network (WWNSS) between 1967 and 1975 (Fig. 8). In Figure 2 selected fault plane solutions of Ritsema (1961), Fitch (1970), Molnar and others (1973), Ben-Menahem and others (1974), and Tapponnier and Molnar (1977) are given in addition to the 5 solutions determined by this study.

The fault plane solutions in central and western Tibet show normal faulting with fault planes striking from northeast to northwest. The mechanisms of August 16, 1973, September 8, 1973, and May 3, 1971 have both normal and strike-slip components. High angle normal faults striking northwest observed on LANDSAT imagery are consistent with the fault plane solutions (Fig. 9a and b).

The earthquake of August 15, 1967 occurred near the numerous northwest trending linear scarps traced from LANDSAT imagery. These fault traces also trend parallel to the Po-Chu Fault. The fault plane solution shows right-lateral motion on it. Further support for right-lateral motion comes from the fault plane solution of the Assam earthquake, August 15, 1950, which was located about 7 km from the Po-Chu fault, although this fault plane solution has been a subject of controversy. Tandon (1955) reported a normal fault plane solution based on the first motion reported in ISS. Chen and Molnar (1977) found that the same ISS data and aftershock is consistent with a shallow dipping underthrust to the north. However, Ben-Menahen and others (1974) have gone through all the available original data regarding first P motion and aftershock locations

and have added surface wave amplitude studies before reporting a right-lateral strike-slip fault plane solution. Their solution is consistent with observed right-lateral motion on the Po-Chu fault (Fig. 5).

The fault plane solution of a large earthquake on January 19, 1975, south of the Karakoram fault, show normal faulting with both nodal planes striking approximately north. Observed normal faults on LANDSAT imagery in this region (Fig. 10) are also consistent with regional east-west extension. Previously determined fault plane solutions in Tibet by Molnar and others (1973) and Tapponnier and Molnar (1977) also show normal faulting striking approximately north. These are also consistent with normal faults observed on LANDSAT imagery (Fig. 2).

CONCLUSION

The data presented show that the net effect of fault movement within the Tibetan Plateau is both crustal compression oriented north-south and crustal extension oriented roughly east-west. The compressional tectonics represented mostly by strike-slip faults, can be simply related to the collision of the Indian and Eurasian plates (Dewey and Burke, 1973; Molnar and Tapponnier, 1975). The principal problems concerning the present tectonics of the Tibetan Plateau are the cause of the east-west trending extensional tectonics and the direction of relative motion between the Indian plate, the Tibet block and the Tarim block.

After the collision of the Indian and Eurasian plates the crust of the Tibetan Plateau has been thickened to 70 to 80 Kilometers by conservation of in flow mass into the collision belt (Arraham and Nur, 1976). This extra thick crust, although presently in near isostatic equilibrium (Shih, 1974), does not represent a mechanical equilibrium position of the crust and the lithosphere (Artyushkov, 1974). Therefore the thickened Tibetan Plateau will seek to reach its equilibrium by flattening out its crust. This process, similar to the gravitational force due to high elevation (McKenzie, 1972), will produce tensional tectonics on the surface of the crust in random directions. Because most of the normal faults observed from the LANDSAT imagery trend in a north-south direction and tensional axes from fault plane solutions tend to be oriented east-west, boundaries around the Tibetan Plateau must strongly influence the direction of flattening. The lines marking the approximate block boundaries around Tibet are schematically shown on Figure 11. The arrows on the plate and blocks show the direction of motion relative to eastern China. The Tibetan Plateau is wedged aside by the north moving Indian plate and it is being

displaced eastward between the right lateral Karakoram fault and left lateral Astin-Tagh fault as envisioned by Molnar and Tapponnier (1975). The eastward movement of the Tibetan Plateau is also due to the least resistence of its eastern boundaries. This observations is supported by the eastward displacement of the continental lithosphere in central China (Molnar and Tapponnier, 1975; Tapponnier and Molnar, 1976). Nevertheless, the eastward movement of the Tibetan Plateau probably is not uniform throughout its entire region. Along a north-south line at about 81°E longitude, concentration of recent volcanism and normal faults distributed along this line (Fig. 2) suggests that the area east of this line is being displaced eastward at a faster rate than the triangular area west of this line. As the north moving Indian plate is continuous through time, one may speculate that rifting of the Tibetan Block is occurring along this line.

Important questions on how much of the Tibetan Plateau has moved eastward and the chemical composition of the recent volcanics and their interrelationships remain unresolved pending further field work. Until more data become available the present model of crustal extension remains premature. Nevertheless, the normal faulting and east-west crustal extension are independent of any model.

Ben-Menahem, A., Aboudi, E., and Schild, R., 1974. The source of the great Assam earthquake - an intraplate wedge motion, Phys. Earth Planet. Int., 9:265-289.

Bird, P., Toksöz, M.N., 1977. Strong attenuation of Rayleigh waves in Tibet, Nature, 266:161-162.

Bonilla, M.G., and Allen, C.R., 1975. Seismotectonics in China, in Earthquake Research in China, Trans. Am. Geophys. Union, 56:853-856.

Burke, K.C., Dewey, J.F., and Kidd, W.S.F., 1974. The Tibetan Plateau: Its significance for tectonics and petrology (abs.), Geol. Soc. America Abs. with Programs, v. 6, no. 7, 1028-1029.

Chang, C., and Cheng, H., 1973. Some tectonic features of Mt. Jolmo Lungma area, southern Tibet, China, Sci. Sinica, 16:257-265.

Chang, T., 1963. The Geology of China (English transl.). U.S. Dept. Commerce Tech. Services, Jt. Pub., Res. Service, 623 p. (original published, 1959).

Chen, W.P., and Molnar, P., 1977. Seismic moments of major earthquakes and the average rate of slip in central Asia, J. Geophys. Res. (in press).

Chinese Academy of Geological Sciences, 1958. Preliminary Stratigraphy of China (in Chinese). Science, Peking, 190 p.

Colchen, M., 1974. Les formations du domaine Tibétan plissé in Recherches géologiques dans l'Himalaya du Nepal, region de Nyi Shang. Paris, Centre Natl. Recherche Sci., Chap. 4.

Dewey, J.F., and Burke, K.C.A., 1973. Tibetan, Vaviscan, and Precambrian basement reactivation: Product of continental collisional orogeny, J. Geology, 81:683-692.

Fitch, T.J., 1970. Earthquake mechanisms in the Himalayan, Burmese, and Andaman regions and continental tectonics in central Asia, J. Geophys. Res., 75:2699-2709.

Ganser, A., 1964. The Geology of the Himalayas, Wiley, Interscience, New York, 289 p.

Geologic Map of China, 1976, Chinese Academy of Geological Sciences, (1:4,000,000), Peking, China.

Gupta, H.K., and Narain, H., 1967, Crustal structure in the Himalayan and Tibet Plateau region from surface wave dispersion, Bull. Seism. Soc. Am., 57:235-248.

Kidd, W.S.F., 1975, Widespread late Neogene and Quaternary calc-alkaline vulcanism on the Tibetan Plateau, EOS, Trans. AGU, 56:453.

Molnar, P., Fitch, T.J., and Wu, F.T., 1973. Fault plane solutions of shallow earthquakes and contemporary tectonics in Asia, Earth and Planet. Sci. Lett., 19:101-112.

Molnar, P., and Oliver, J., 1969. Lateral variations of attenuation in the mantle and discontinuities in the lithosphere, J. Geophys. Res., 74:2648-2682.

Molnar, P., and Tapponnier, P., 19 . Cenozoic tectonics of Asia: Effects of a continental collision, Science, 189:419-426.

Powell, C. McA. and Conaghan, P.J., 1975. Tectonic models of the Tibetan Plateau, Geology, 3:727-731.

Ritsema, A.R., 1961. Some 1951 earthquake mechanisms based on P and PkP data, Geophys. J. R. Astron. Soc., 5:254-258.

Rugiakin, A.I., Nersesov, I.L., Khalturin, V.Z., and Molnar, P., 1977, Propagation of Lg and lateral variations in crustal structure in Asia, J. Geophys. Res., 62:307-316.

Segor, A.M.C., 1976. Collision of irregular continental margins: Implications for foreland deformation of Alpine-type orogens, Geology, 4:779-782.

Shih, C.L., Huan, W.L., Wu, H.R., and Cao, X.L., 1973. On the intensive seismic activity in China and its relation to plate tectonics (in Chinese), Scientia Geol. Sinica, 4:281-293.

Shih, C.L., Huan, W.L., Yao, K.K., and Hsie, Y.T., 1974. On the fracture zones of Changma earthquake of 1932 and their causes, Acta Geophys. Sinica, 17:272-290.

Tandon, A.N., 1955. Direction of faulting in the great Assam earthquake of August 15, 1950, Ind. J. Meteor. Geophys., 6:61-64.

Tapponnier, P., and Molnar, P., 1976. Slip line field theory and large-scale continental tectonics, Nature, 264:319-324.

Tapponnier, P., and Molnar, P., 1977. Active faulting and Cenozoic tectonics in China, J. Geophys. Res. (in press).

Teng, C.W., and others, 1974. Deep reflected waves and the structure of the earth crust of the eastern part of Tsaidam basin (in Chinese), Acta Geophys. Sinica, 17:122-135.

Tung, J.P.Y., 1975, The surface wave study of crustal and upper mantle structures of mainland China, Ph.D. Thesis, Univ. of Southern California, 331 p.

York, J.E., Cardwell, R., and Ni, J., 1976. Seismicity and Quaternary faulting in China, Bull. Seism. Soc. Am., 66:1983-2001.

FIGURE CAPTIONS

Figure 1: Physical and tectonic features of the Tibetan Plateau and surrounding regions.

Figure 2: Seismo-tectonic map of the Tibetan Plateau. Faults and type of faulting are interpreted from LANDSAT imagery. Solid arrows indicate direction of motion supported by fault plane solutions or surface faulting of earthquakes from Molnar and Tapponnier (1975) and York and others (1976). Open arrows indicate direction inferred from photo interpretation above. Large open circles represent all selected earthquakes (see text) with $5 \leq M \leq 6\text{-}1/4$; small open circles, $4 \leq M < 5$. The numbered 1 through 5 fault plane solutions correspond to events reported in Figure 8. Previously reported solutions are indicated by letters next to the solutions. R is from Ritsima (1961), F from Fitch (1970), M from Molnar and others (1973), B from Ben-Menahem and others (1974), and T from Tapponnier and Molnar (1977). Solid areas indicate Neogene to Quaternary volcanis interpreted from LANDSAT imagery.

Figure 3: (a) Arrows indicate normal faults in the left portion of the photo. Notice the horst and graben feature and sharp tonal and textural contrast across the fault. Center of image is approximately 31.5°N, 82.5°E.
(b) N-S striking normal faults indicated by arrows on eastern flank of the graben at the center of the photo. Its broken but short, linear trace is clearly seen here. At A the intruded granite (Tertiary age) is offset by the fault. The V-shaped streams and strong tonal difference across the fault are clearly seen. Center of image is approximately 28.8°N, 86.4°E.
(c) Basin and Range province, southeastern California. Arrows indicate the strike-slip Garlock fault. The pattern of known normal faults is similar to that seen in Tibet. Center of image is approximately at 32.6°N, 117°W.

Figure 4: An apparently dammed lake along section of the Asting-Tagh fault, apparently formed within grabens associated with the splaying of the main fault into several branches. Center of image is approximately at 38.4°N, 90.5°E.

Figure 5: LANDSAT mosaic of Po-Chu fault (named after Po-Chu River). The name of this fault is not official. The Po-Chu River follows fault along short straight segments. Fault scarp at S and L. Center of image is approximately at 29.3°N, 95.8°E.

Figure 6: (a) Volcano at D and E and well eroded volcano at C. Center of image is approximately 89.425°E and 35.725°N.

(b) Dissected flow sheets at A and B. Drainage has developed atop both mesas indicating that they may be older than Quaternary. Volcanic butte at D. Snow-covered anomalous features around G and H may be Quaternary volcanoes. Center of image is approximately at 35.5°N, 89.4°E.

(c) Quaternary volcano at V. Center of image is approximately at 38.7°N, 89.6°E.

Figure 7: Miocene basalt and rhyolite flows at A, B and C in New Mexico, U.S.A. from Geologic Map of New Mexico (1965). Center of image is approximately at 33.5°N, 106.2°W.

Figure 8: New focal mechanism solutions for crustal earthquakes in Tibet, using lower hemisphere projections. Polarities of P-wave first motions are given by large and small solid circles for clear and weak compression, respectively; large and small open circles for clear and weak dilatation, respectively; and crosses for uncertain polarization. S-wave polarization is indicated by arrows. Tick marks on nodal planes give the locations of poles to one of the nodal planes. P and T are the location of maximum and minimum compression, respectively.

Figure 9: (a) Earthquake of May 3, 1971 and its fault plane solution. Arrows indicate normal faults. Center of image is approximately at 32.8°N, 87.3°E. (b) Earthquakes of August 16, 1973 and September 8, 1973 and their fault plane solution. Arrows indicate normal faults in nearby areas. A domal feature is located at D and a circular lake at C. Center of image is approximately at 32.8°N, 87.3°E.

Figure 10: Earthquake of January 19, 1975 and its fault plane solution. Young alluvial fan has formed along fault scarp at F. Arrow points to the N-S trending normal fault. Karakoram fault lies between arrows. Center of image is approximately at 33°N, 78.8°E.

Figure 11: Schematic map showing tectonic interpretation. Broad line indicates approximate plate and block boundaries. Large arrows show relative motion between the Tibetan block, Tarim block and the Indian plate.

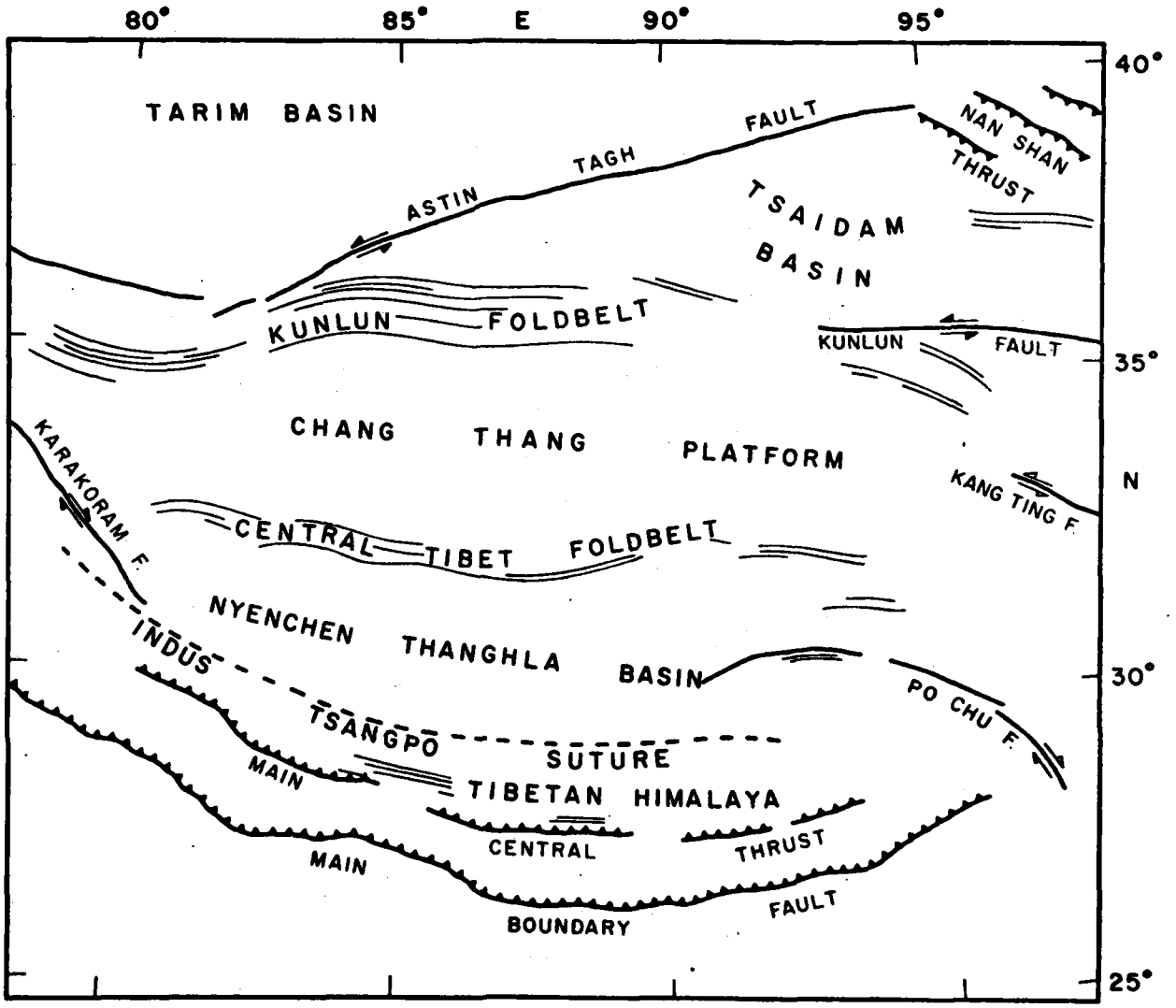
80°
85°
E
90°
95°
40°
35°
30°
25°
N
TARIM BASIN
ASTIN
TAGH
FAULT
NAN SHAN
THRUST
TSAIDAM
BASIN
KUNLUN
FOLDBELT
KUNLUN
FAULT
CHANG
THANG
PLATFORM
KARAKORAM F.
KANG TING F.
CENTRAL
TIBET
FOLDBELT
NYENCHEN
THANGHLA
BASIN
INDUS
TSANGPO
SUTURE
PO CHU F.
MAIN
TIBETAN HIMALAYA
CENTRAL
THRUST
MAIN
FAULT
BOUNDARY

Figure 1

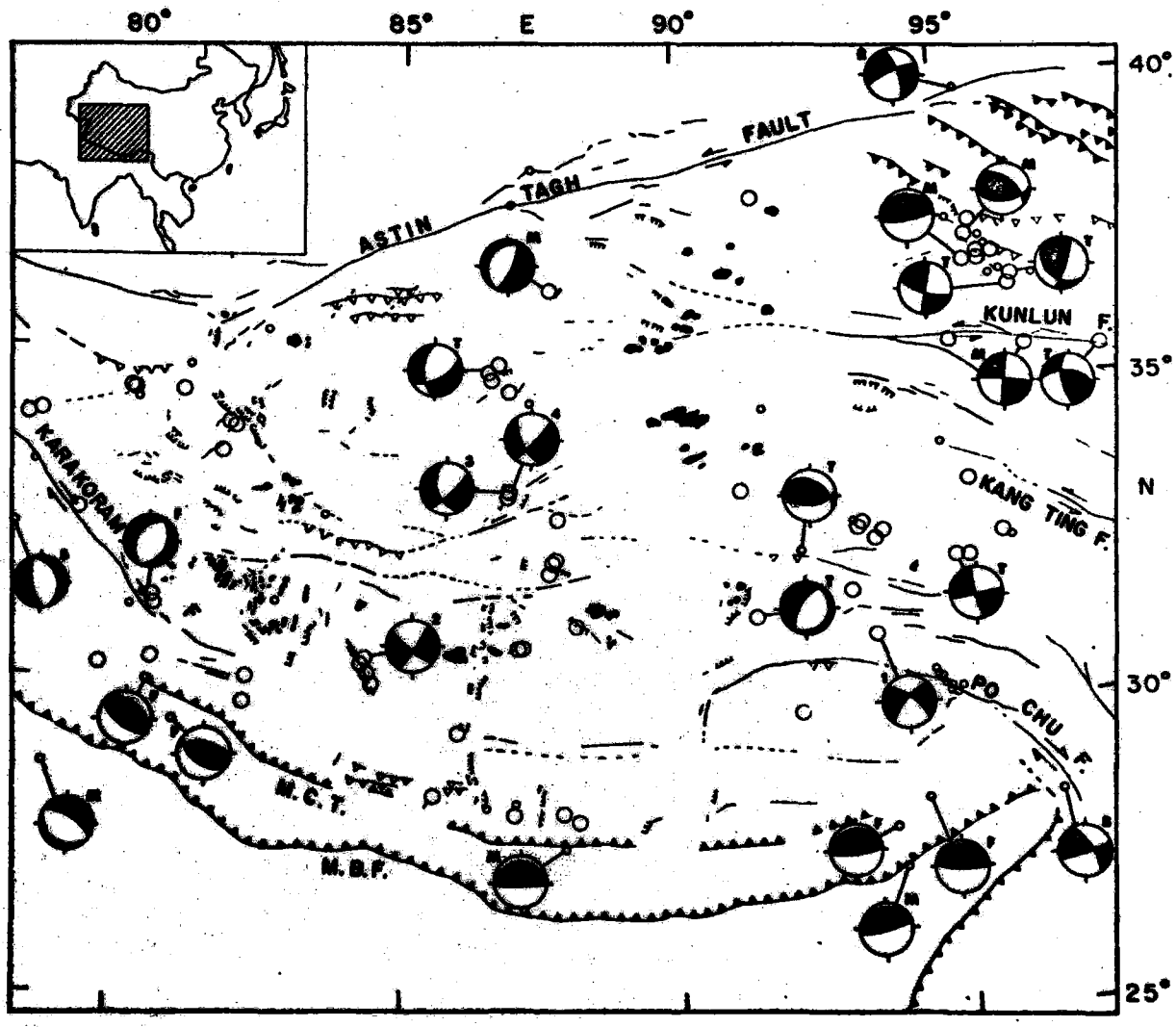
80°
85°
E
90°
95°
40°
35°
N
30°
25°
FAULT
ASTIN
TAGH
KUNLUN F.
KARAKORAM
KANG TING F.
PO CHU F.
M.C.T.
M.B.F.

Figure 2

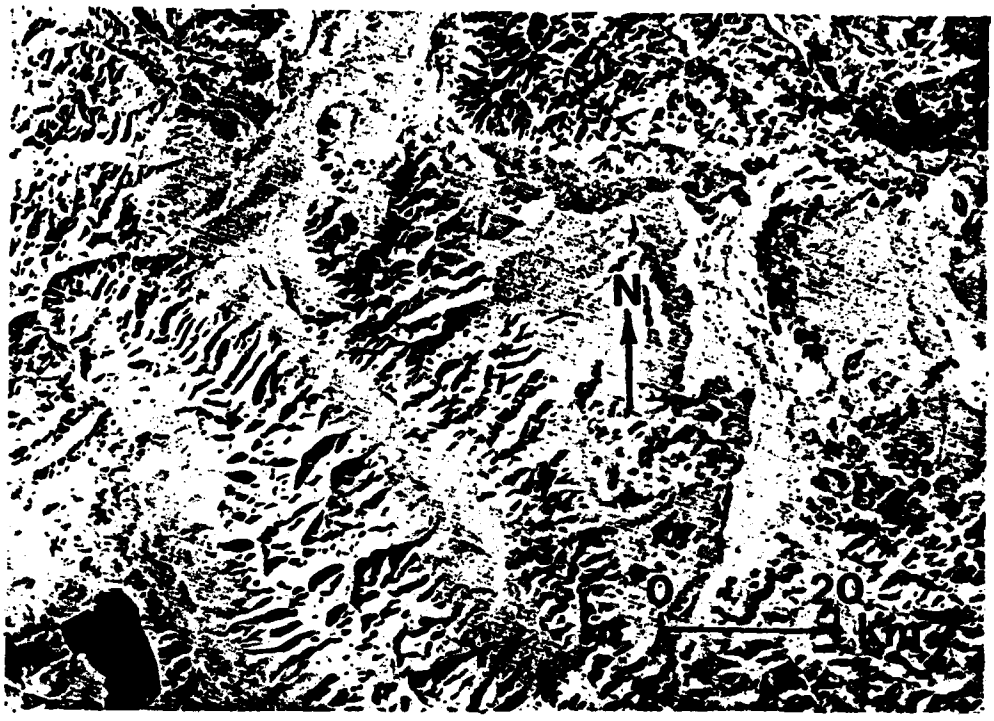

Figure 3a

Figure 3b

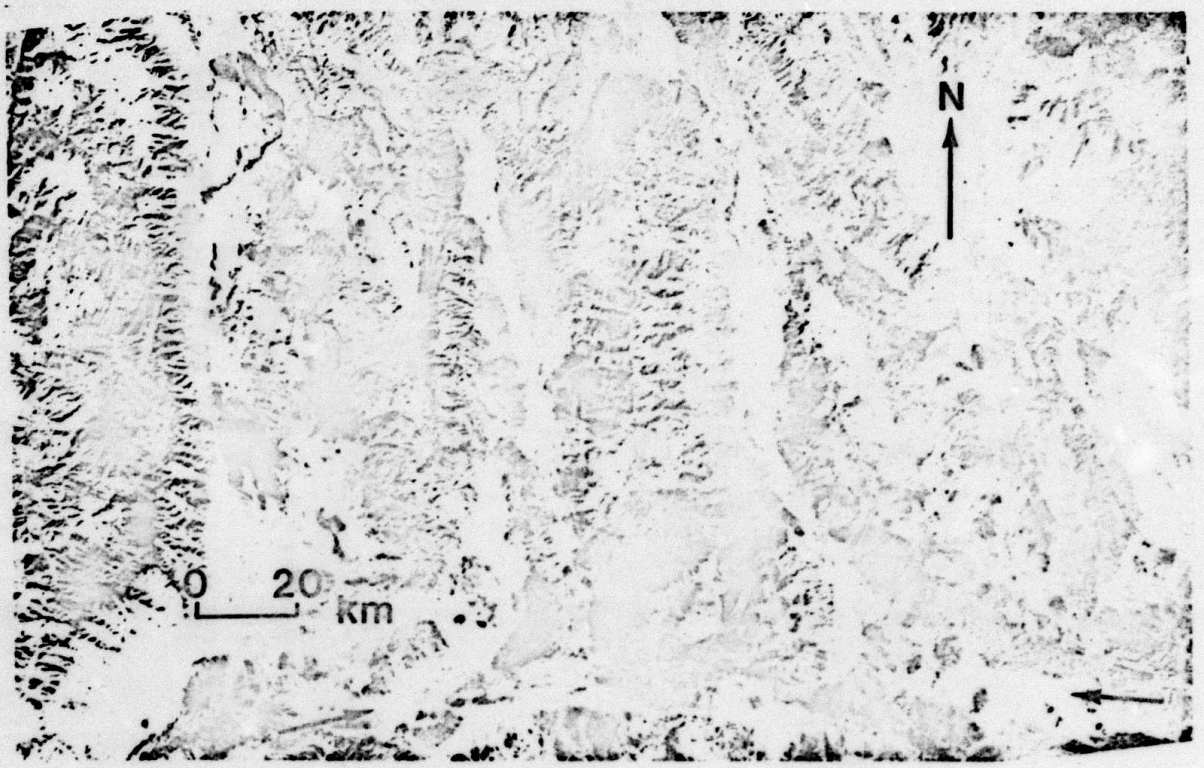

Figure 3c

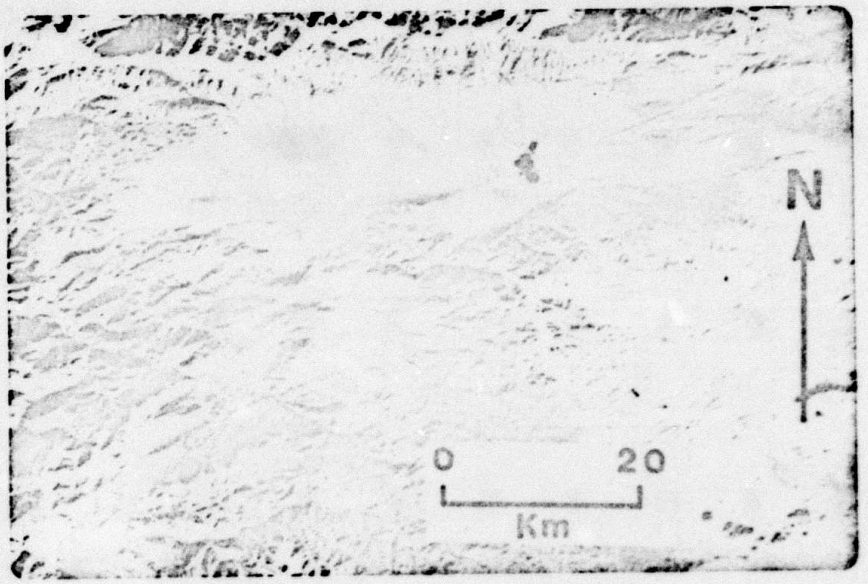

Figure 4

Figure 5

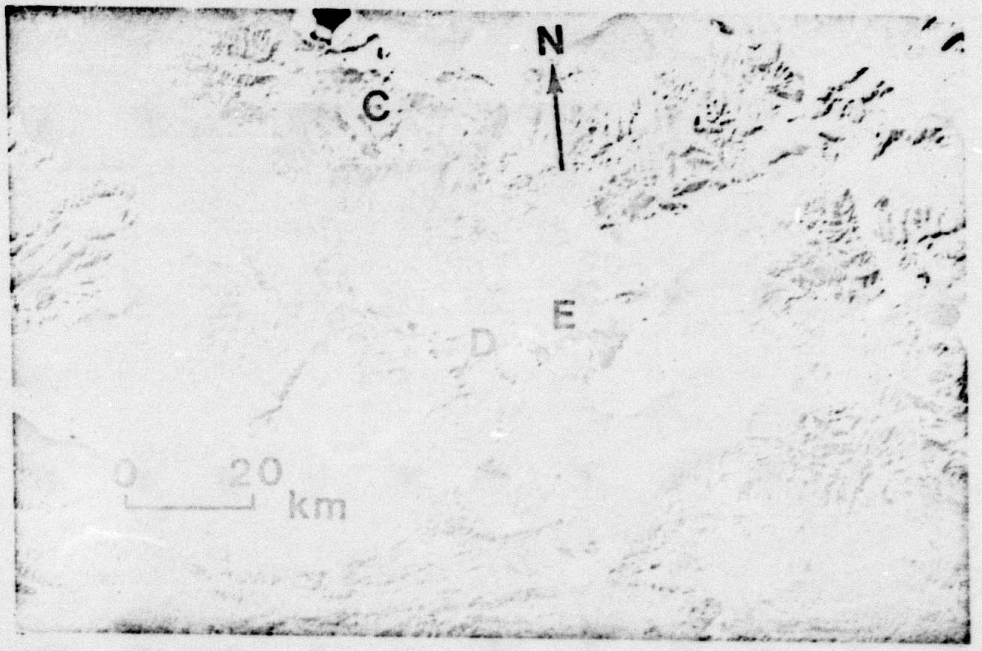

Figure 6a

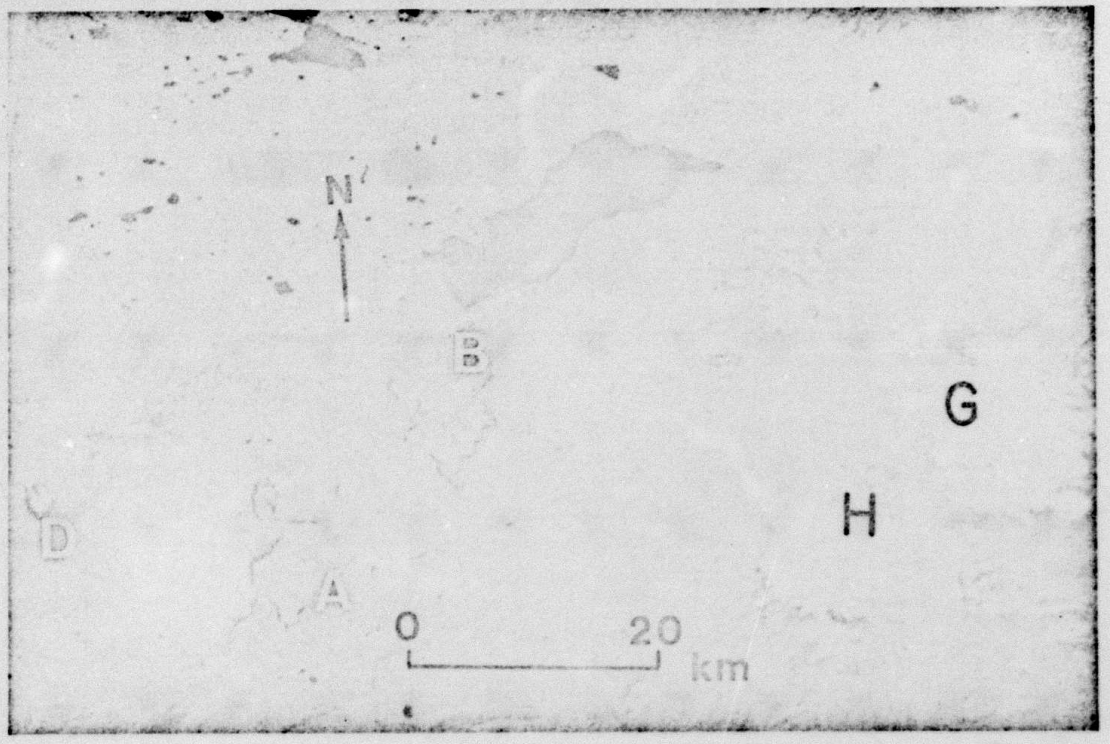

Figure 6b

Figure 6c

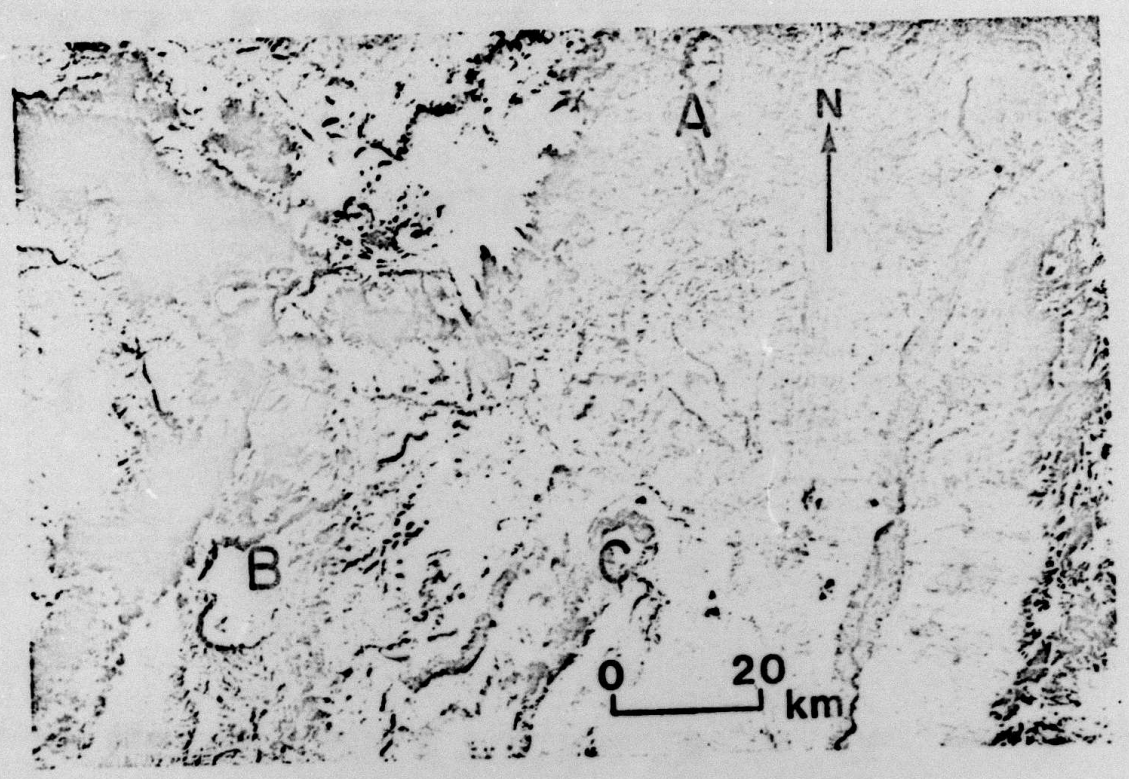

Figure 7

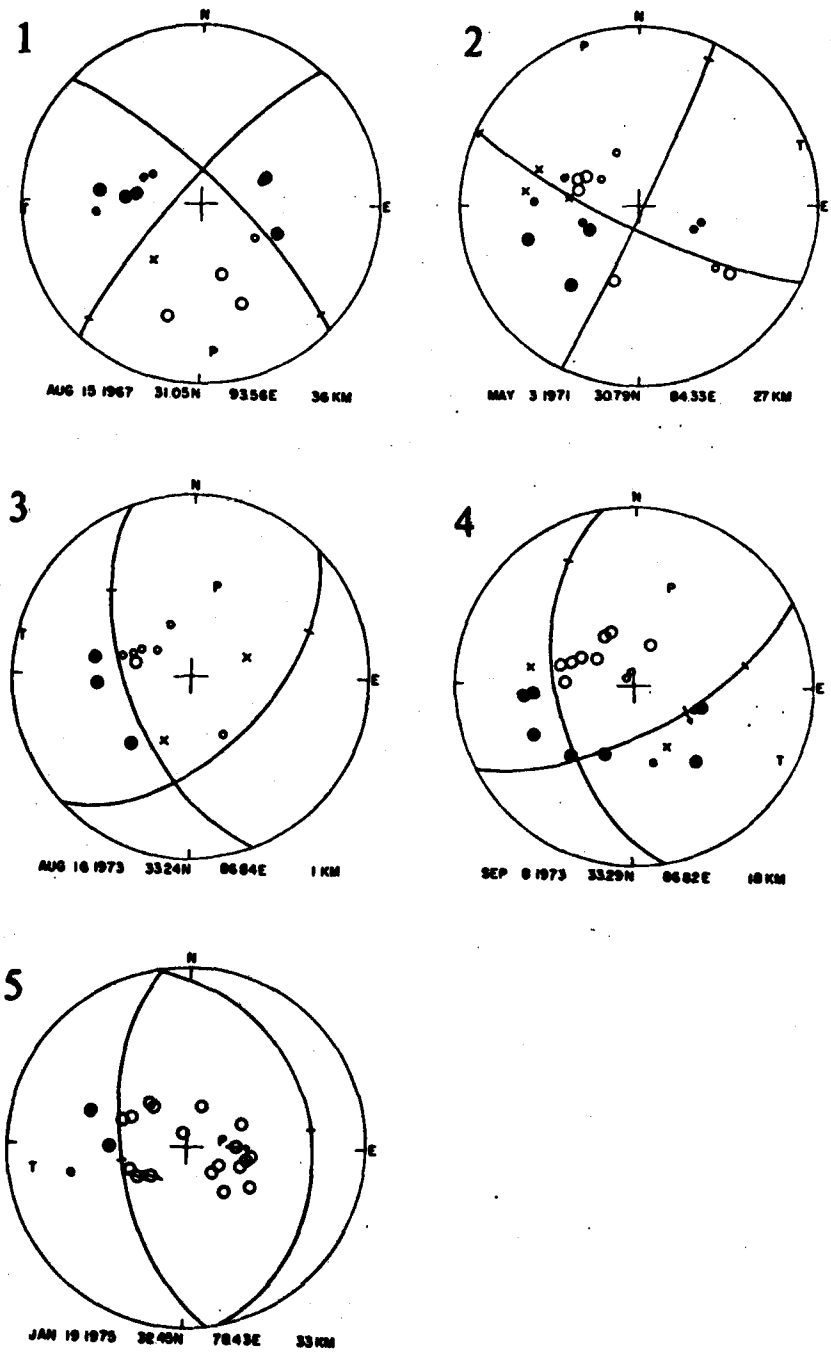
1
N
E
P
AUG 15 1967 31.05N 93.56E 36 KM
2
N
P
T
E
MAY 3 1971 30.79N 84.35E 27 KM
3
N
P
T
E
AUG 16 1973 33.24N 86.64E 1 KM
4
N
P
E
T
SEP 8 1973 33.29N 86.82E 10 KM
5
N
T
E
JAN 19 1975 32.48N 78.43E 33 KM

Figure 8

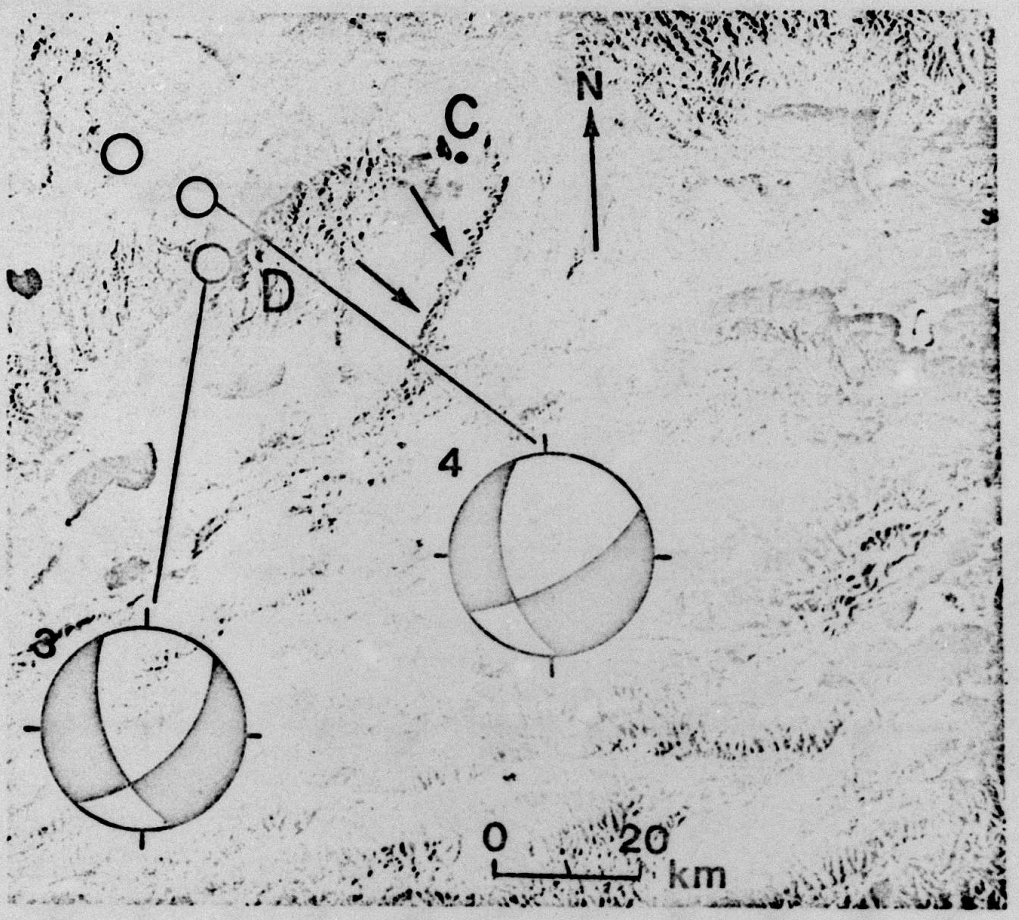

Figure 9a

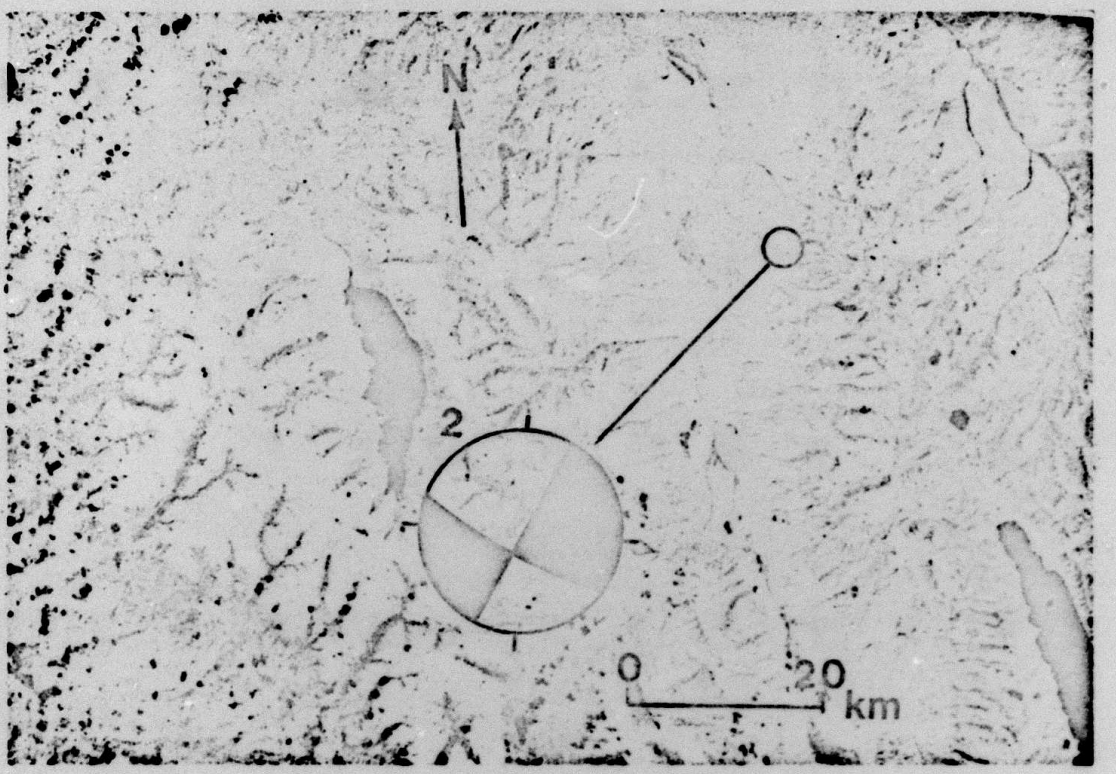

Figure 9b

Figure 10

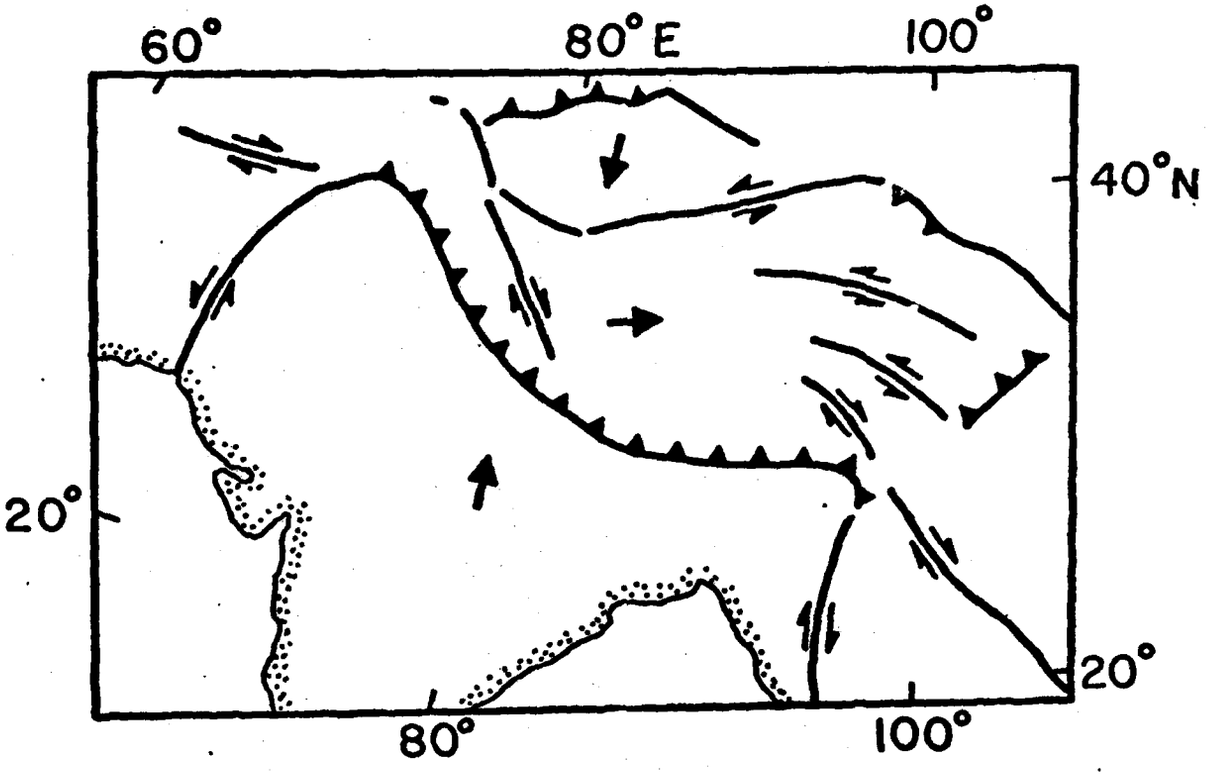

Figure 11

Relocation of the Tien Shan Events with Joint Hypocenter Determination

A series of earthquakes occurred in the eastern Tien Shan during 1969 and 1971 (Figure 1). These earthquakes are mainly of the shock-aftershock sequence type because of the relatively large magnitude of the main shock compared with the magnitude of the aftershocks. The method of Joint Hypocenter Determination (JHD) was used to relocate the epicenters of the earthquakes. The relocations were obtained with this method using a station-corrected calibration event, initial earthquake hypocenters, initial arrival time, and station arrival times of the events, all taken from the Bulletin of the International Seismological Centre. Thirty earthquakes were relocated by this method with a maximum of 15 possible stations per earthquake and a minimum of seven stations per earthquake. Stations were chosen to give the best possible uniform azimuthal and epicentral coverage as well as the most reliable readings. Table 1 gives the station epicentral distances and approximate azimuths.

The ISC reported depths for most of these events less than 47 km. These depth determinations are calculated from arrival times of P only. Thus, without pP data or arrival times at stations very close to the source, it is impossible to accurately determine focal depths. Since our primary interest is to develop reliable techniques to determine fault planes along with fault plane solutions and satellite imagery, approximation is made by assuming all hypocenters to be at the same depth. The resulting relocated epicenters are shown in Figure 2. The dotted lines represent the approximate trend of aftershocks. This trend is in good agreement with the "A" nodal plane also shown in Figure 2. Therefore, this nodal plane, which strikes N75°W with a shallow north-dipping angle, is chosen for the fault plane.

Interpretation of LANDSAT imagery indicates no obvious lineament trending in this direction. However, the approximately east-west folding in the foothills of the Tien Shan indicates a shallow thrusting dip toward the north. This observation is also in agreement with the general trend of the aftershock sequences. Further study of LANDSAT imagery of different seasons is necessary to determine whether faults can be observed from the imagery.

TABLE 1.

Stations Used in the JHD Relocations

Station Abbreviation	Epicentral Distance (deg)	Azimuth (deg)
PRZ	1.19	331
MNL	9.33	209
KBL	10.55	323
NDI	12.83	188
QUE	15.18	226
SHL	18.87	143
GBA	27.69	185
NUR	38.16	319
NIE	41.29	302
KRA	41.31	303
GRF	47.08	304
MBC	62.00	5
COL	67.80	20
YKC	75.84	7
WRA	79.34	129

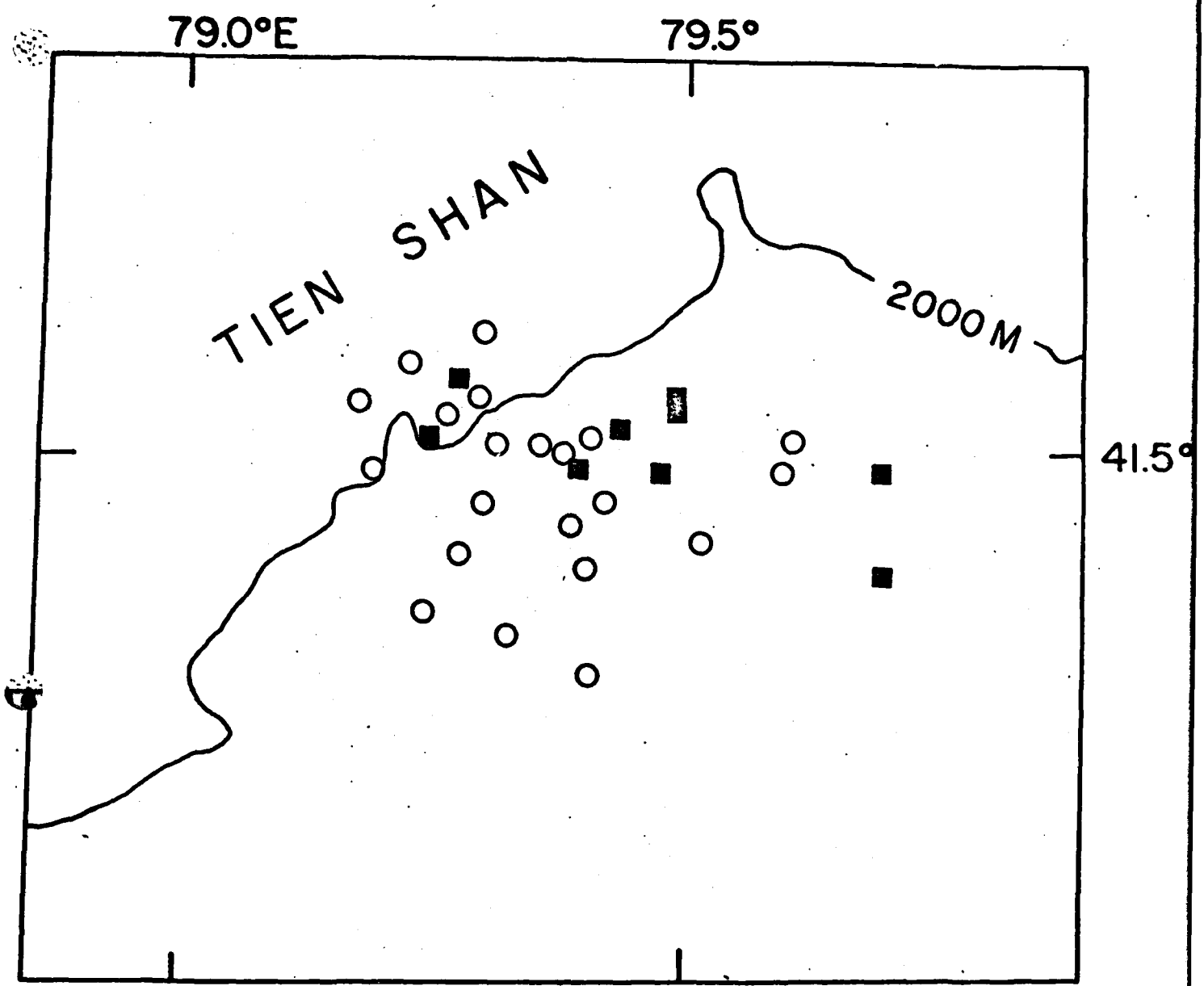

Figure 1. Map shows ISC location of epicenters from 1969 to 1971 events. Solid squares represent 1969 aftershock sequence, open circles represent 1971 aftershock sequence.

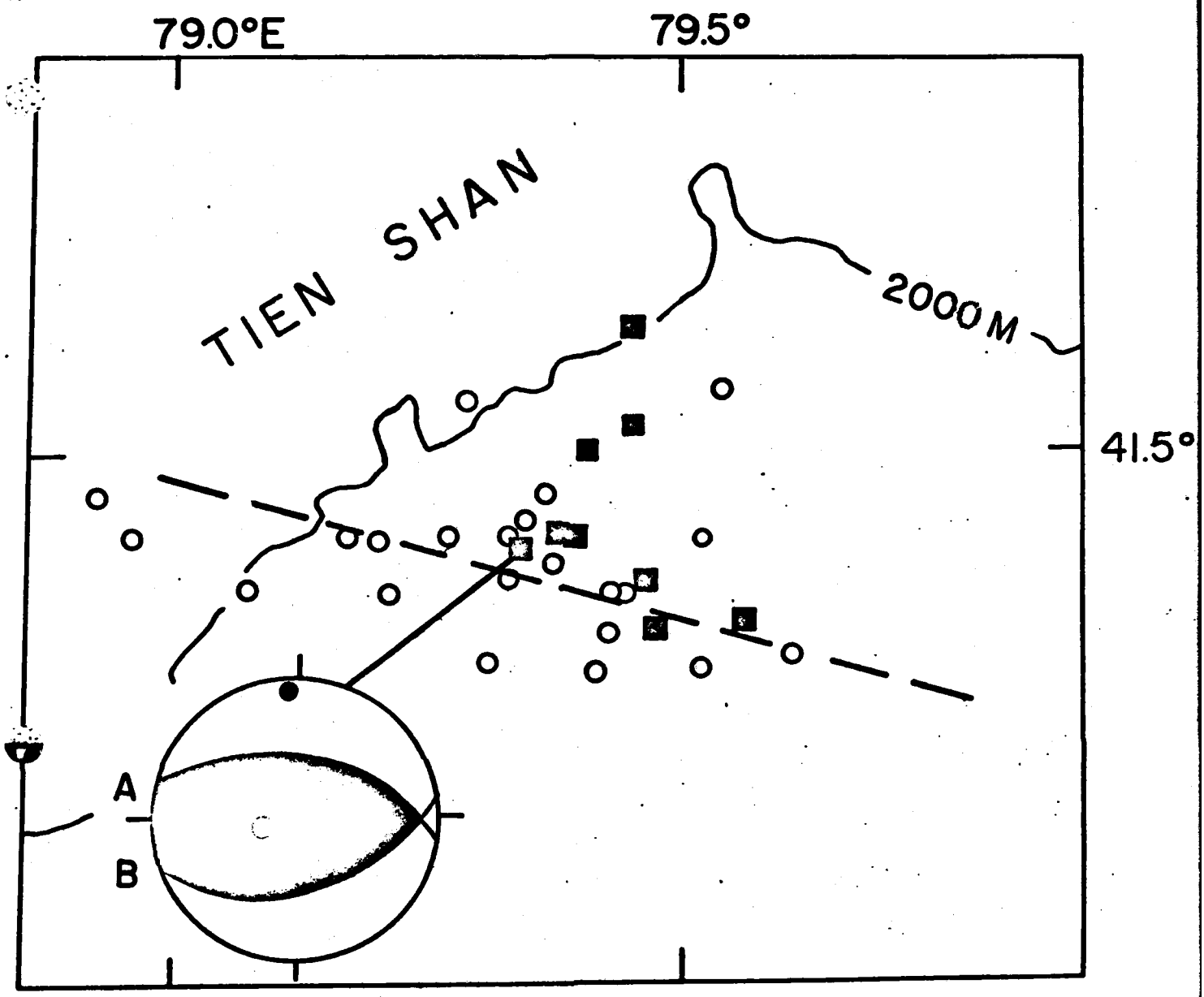

Figure 2. Map shows JHD relocated epicenters from 1969 to 1971 events. Solid squares represent 1969 aftershock sequence, open circles represent 1971 aftershock sequence. Fault plane solution of February 2, 1969 events is taken from Molnar et al., 1973.

Fault Plane Solution of Haicheng Earthquake of February 4, 1975

A major earthquake occurred in the Liaoning province on February 4, 1975. The USGS has reported the following parameters for this earthquake:

epicenter: latitude 40.641°N, longitude 122.58°E
origin time: 11 hours, 36 minutes and 7.54 seconds
depth of focus: normal
magnitude: 7.4 (MS)

Data for this earthquake were obtained through WWNSS stations. Only the first motion of P waves and some S wave polarizations recorded on the long-period instruments are used in the construction of the fault plane solution. The mechanism (Figure 1) indicates strike-slip faulting. This earthquake was accompanied by numerous aftershocks. Figure 2 shows the distribution of earthquakes of magnitude 2 and greater between February 1 and May 31, 1975 (Gu and others, 1976). Aftershocks were concentrated in an area 70 km long and 30 km wide and the epicentral depth distribution was between 1 and 17 km with most less than 12 km. Therefore, we conclude that the near-vertical east-west trending nodal plane is the fault plane.

Reference:

Gu, H.D., Chin, Y.T., Gao, X.L., and Zhao, Y., 1976, Focal mechanism of the Haicheng, Kiaoning Province, earthquake of February 4, 1975, Acta Geologica Sinica, 19:270-284.

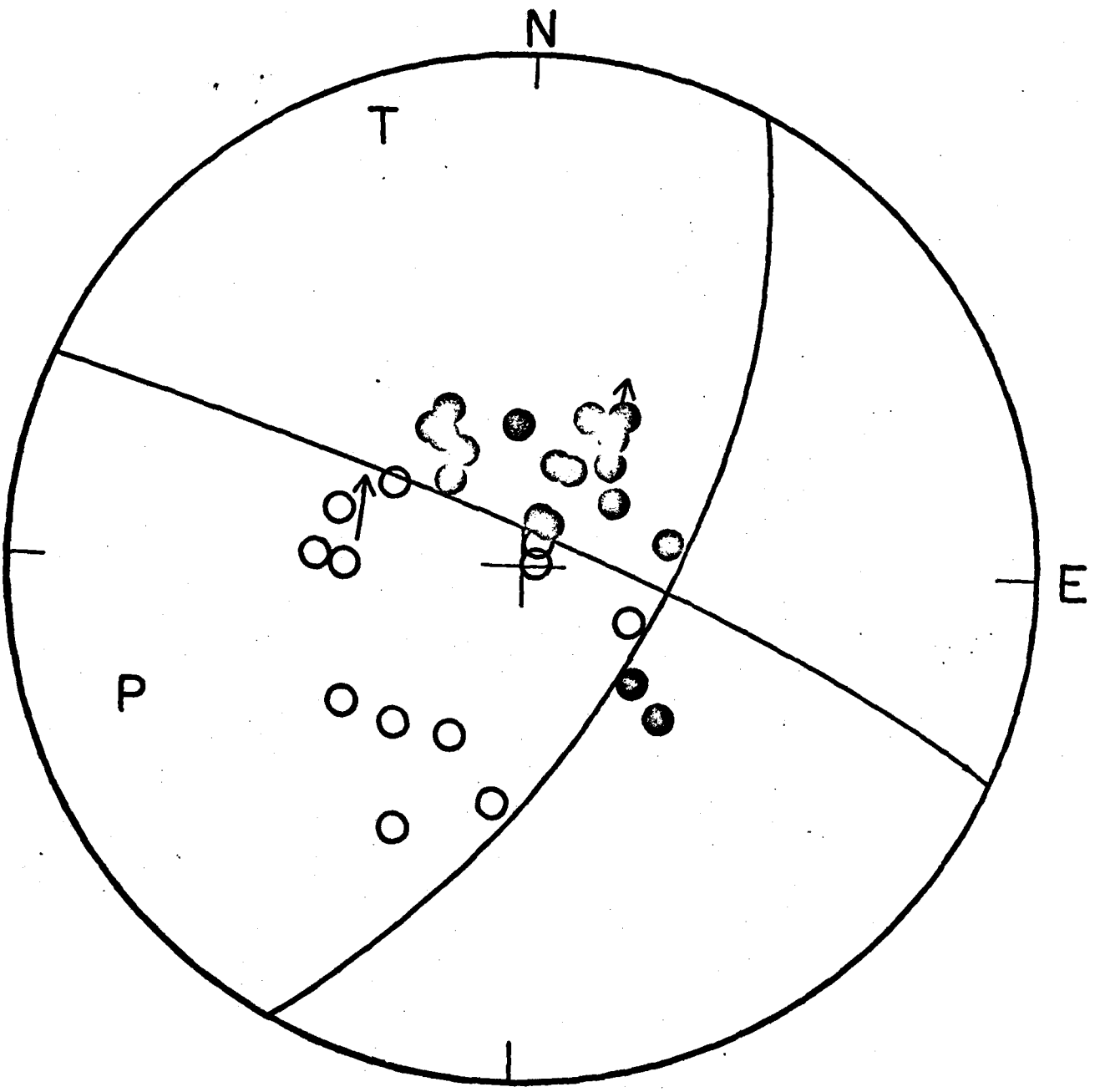

Figure 1. Focal mechanism using lower hemisphere projections. Polarities of P wace first motion are given by solid circles, open circles for dilatation. S-wave polarization is indicated by arrows. P and T are the location of maximum and minimum compression, respectively.

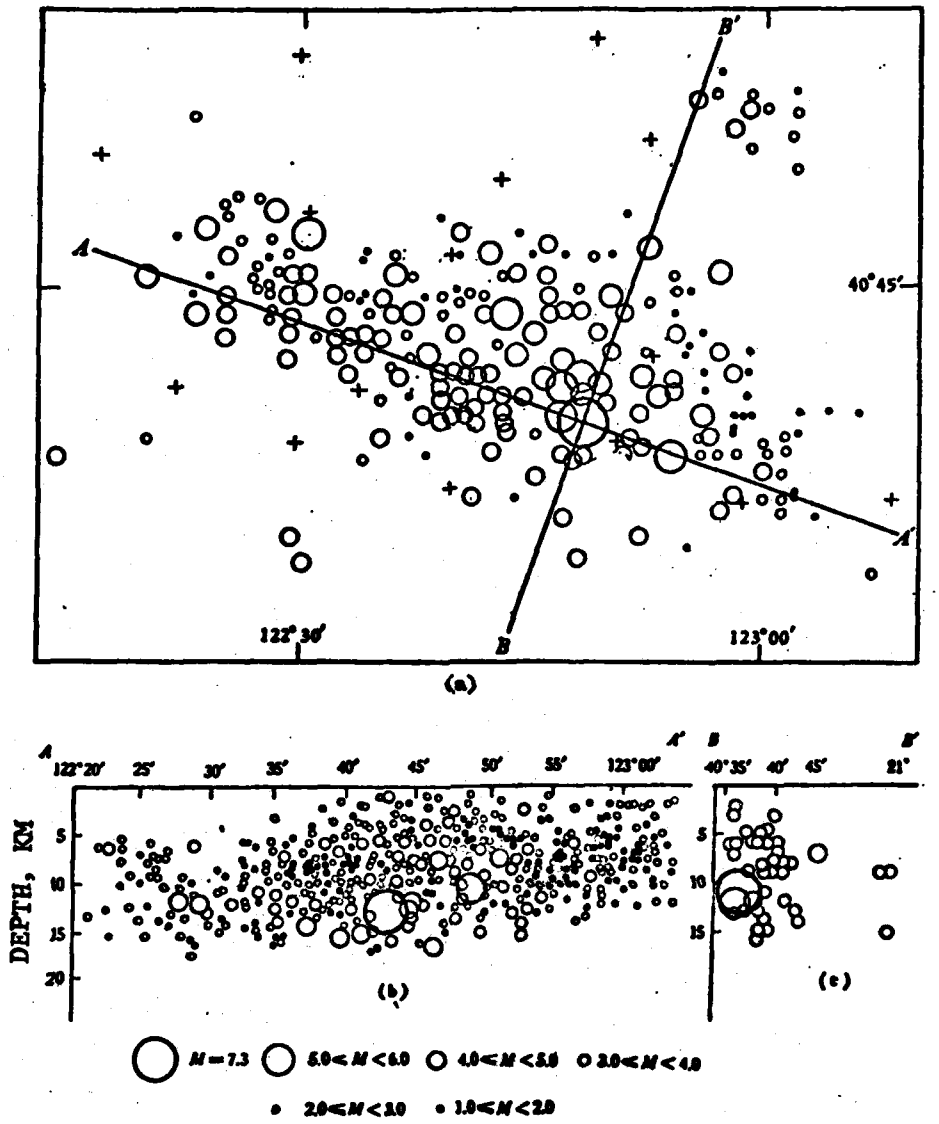

Figure 2. Map shows the distribution of earthquakes of magnitude 2 and greater between February 1 and May 31, 1975 from Gu and others, 1976.